Chapter

Invasiveness-Related Proteomic Variations and Molecular Network Changes in Human Nonfunctional Pituitary Adenomas

Xianquan Zhan, Xiaohan Zhan and Xiaowei Wang

Abstract

The invasive characteristic of nonfunctional pituitary adenoma (NFPA) is an important clinical problem without a clear molecular mechanism, which severely challenges its treatment strategy. Clarification of the proteomic alterations between invasive and non-invasive NFPAs is the key step for in-depth understanding of its mechanisms and discovering reliably invasive biomarkers. Two-dimensional gel electrophoresis (2DGE)-based comparative proteomics was carried out between four invasive and four non-invasive NFPAs. A total of 64 upregulated protein-spots and 39 downregulated protein-spots were identified among 24 (invasive n = 12; non-invasive n = 12) 2DGE maps (ca. 1200 spots/gel). Mass spectrometry identified 30 upregulated proteins and 27 downregulated proteins between invasive and non-invasive NFPAs. Those 57 differentially expressed proteins are involved in multiple biological functions, including oxidative stress, mitochondrial dysfunction, MAPK signaling alteration, proteolysis abnormality, CDK-C signaling, amyloid processing, and TR/RXR activation. These findings provide important clues to insights into molecular mechanisms of invasive NFPAs and to discovery of effective biomarkers for effective treatment of invasive NFPA patients.

Keywords: invasive nonfunctional pituitary adenoma, two-dimensional gel electrophoresis, mass spectrometry, proteome, comparative proteomics, invasive biomarker

1. Introduction

Invasive pituitary adenoma is a type of pituitary adenoma that locally invades contiguous anatomy structures surrounding pituitary gland [1–6]. In fact, the rate of local invasion is about 40% of pituitary adenoma patients with macroscopic observation, and even up to 80% of pituitary adenoma patients with microscopic observation [1, 7, 8] although most pituitary adenomas are align. Magnetic resonance imaging (MRI) is commonly used method to measure the size of pituitary adenomas, and can classify pituitary adenomas into giant adenomas (>40 mm), macro-plus adenomas (20–30 mm), macroadenomas (10–20 mm), and microadenomas (<10 mm) [5, 7]. Furthermore, based on preoperative MRI and perioperative observation, pituitary adenomas are classified into grade I (enclosed

microadenoma, <10 mm), grade II (enclosed macroadenoma, >10 mm), grade III (localized perforation of the sellar floor), and grade IV (diffuse destruction of the sellar floor) [9]. Grades III and IV are commonly looked as invasive pituitary adenomas. Invasiveness is very challenging clinical problem in pituitary adenoma patient, which reasons are that (1) invasiveness suppresses and/or damage surrounding structures because of the limited intracranial cavity and around important structure tissues, and (2) invasiveness causes incomplete removal of pituitary adenoma in neurosurgery to increase risks of complications including recurrence and poor outcome and need adjuvant therapy (radiotherapy or medications) [1]. However, the molecular mechanisms of pituitary adenoma invasiveness remain unclear, although some studies [10] found more vascular evidence in invasive pituitary adenomas compared to non-invasive tumors to indicate the role of angiogenesis [10], and some molecular and genetic changes in invasive pituitary adenomas including downregulation and methylation of CDH13 (H-cadherin) and CDH1 (E-cadherin) [11], loss of death-associated protein kinase and CpG island methylation [12], and loss of heterozygosity at 11q13 (MEN1 locus) and 13q (retinoblastoma gene RB locus) without mutation and overexpression of p53 and without homozygous deletions of p15 or p16 [13]. Multiomics analysis is an effective approach to investigate systematically molecular mechanisms of invasiveness of pituitary adenomas [14–19]. Quantitative transcriptomics analysis [9, 20] identified differentially expressed gene (DEG) profiling (346 DEGs, including 233 upregulated and

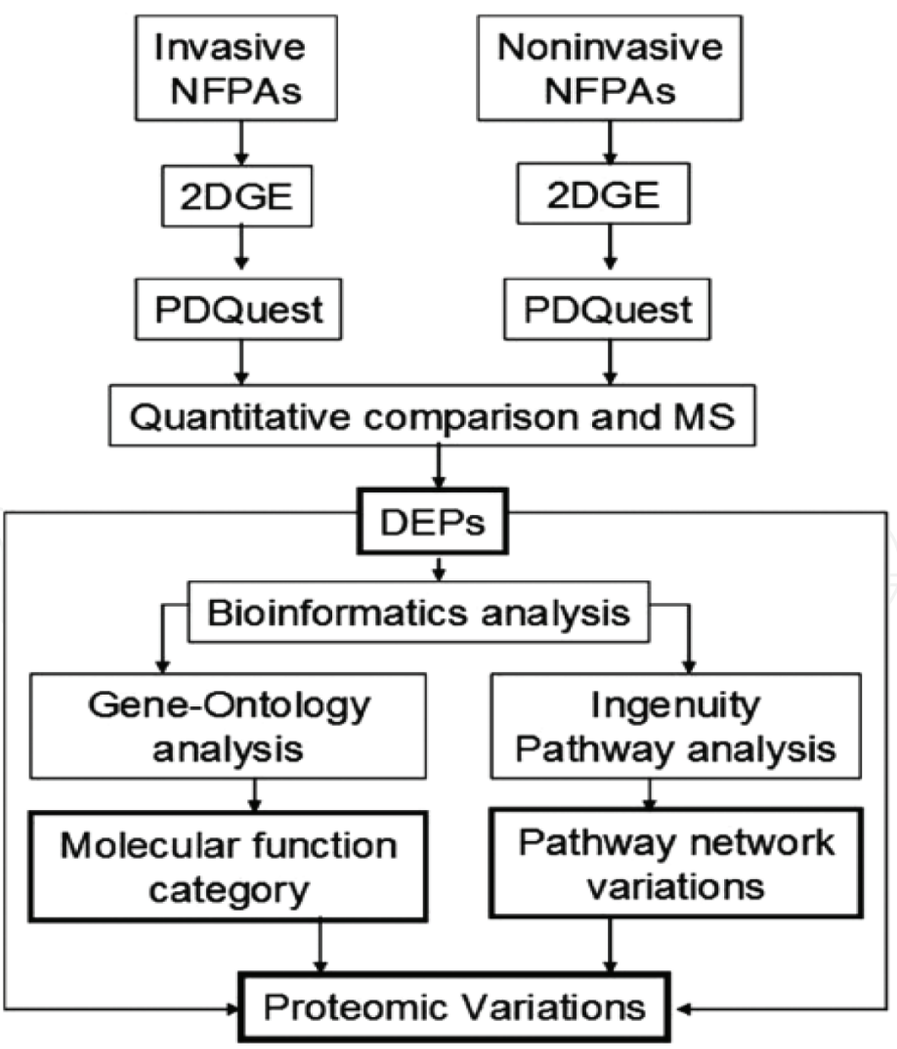

Figure 1.
Experimental flow-chart to comparatively study the proteomes between invasive and non-invasive NFPAs. Reproduced from Zhan et al. [5], with copyright permission from Wiley-VCH, copyright year 2014.

113 downregulated) between invasive and non-invasive NFPAs. However, protein and its proteoforms are the functional performer of each gene, proteome is much more complex than transcriptome, and the coefficient of correlation is very low (about 0.4) in consistence analysis between proteome and transcriptome for the same tissue sample [21, 22]. Therefore, it is necessary to use proteomics for pituitary adenoma invasiveness [23, 24]. A comparative proteomics experiment revealed 30 differentially expressed proteins (DEPs) profiling between invasive and non-invasive pituitary adenoma tissues [25], however, this study did not distinguish the functional and non-functional pituitary adenomas (FPAs, and NFPAs). This chapter focused on the proteomic variations and molecular network changes in invasive relative to noninvasive NFPAs, investigated with two-dimensional gel electrophoresis (2DGE) coupled with mass spectrometry (MS) and pathway network analysis. The findings offer the scientific data to discover protein biomarkers for effective treatment of invasive NFPAs. An experimental flow-chart is shown to study proteomes between invasive and noninvasive NFPAs (**Figure 1**).

2. Materials and methods

2.1 2DGE analysis of pituitary adenoma specimen

The invasive (n = 4) and non-invasive (n = 4) NFPA tissues with pathological diagnosis were used in this study. Each tissue sample was used to individually extract proteins, and the protein content was quantified. Each tissue sample was analyzed with 2DGE for 3–4 times [5, 22]. For each 2DGE analysis, 150 μg proteins were used for isoelectric focusing (IEF) with IPG strips pH 3–10 NL (180 × 3 × 0.5 mm). After IEF, the proteins was reduced and alkalized, and then were separated with the 12% PAGE resolving gel (250 × 215 × 1.0 mm), followed by visualization with modified silver-staining [26]. The PDQuest 2D gel analysis software (version 7.1.0; Bio-Rad) was used to digitize and compare 2DGE gel images between invasive and non-invasive NFPAs. A total of 12 gel images for invasive NFPAs and 12 gel images for non-invasive NFPAs were used in this analysis to determine each DEPs with a 3-fold cutoff values and $p < 0.05$. In addition, four standard proteins, including myoglobin (17 kDa; p. 7.6), carbonic anhydrase (29 kDa; p. 7.0), ovalbumin (45 kDa; p. 5.1), and amyloglucosidase (89/70 kDa; p. 3.8), were applied to measure the observed p*I* and *Mr* on the 2D gel.

2.2 Mass spectrometry analysis of 2DGE-separated proteins

The protein that contains in gel spot was digested in-gel with trypsin, followed by ZipTipC18 purification [5, 26]. For LC-ESI-MS/MS analysis, the purified tryptic peptides were eluted in 6 μl of 85% acetonitrile plus 0.1% TFA, air-dried, and then resuspended in 6 μl of 85% acetonitrile plus 0.1% formic acid. The prepared peptide samples were analyzed by LC-ESI-qTOF mass spectrometer to obtain MS/MS spectrum. For MADI-TOF-MS analysis, the ZipTipC18 peptides were directly eluted on MALDI plate with 2 μl of a-cyano-4-hydroxycinnamic acid solution (seven cycles), and dried, and then were analyzed with Voyager DE STR MALDI-TOF mass spectrometer to obtain peptide mass fingerprint (PMF). The MS/MS data and PMF data were used to search SwissProt database with Mascot software for protein identification.

2.3 Bioinformatics

The software NIHDAVID (version 6.7, http://david.abcc.ncifcrf.gov/summary.jsp) was used to carry out gene-ontology (GO) analysis, including cellular

components (CC), molecular functions (MF), and biological processes (BP), and furtherly were categorized into different functional clusters. Ingenuity pathway analysis (IPA) (www.ingenuity.com) [27] was applied to obtain statistically significant signaling pathways with identified DEP data between invasive and non-invasive NFPAs.

3. Results and discussion

3.1 2DE pattern and DEP profile between invasive and noninvasive NFPA proteomes

Each NFPA tissue sample (four invasive NFPAs and four non-invasive NFPAs) was analyzed by 2DGE for 3–5 times to guarantee at least three high-quality gel images. Thus, 24 high-quality 2DGE images (12 gel-images for invasive NFPAs; 12 gel images for non-invasive NFPAs) were obtained. About 1200 spots (an average of 1172 spots for invasive NFPAs and 1213 spots for non-invasive NFPAs) were present in each gel image (**Figure 2**), and most of spots were distributed within pH 4–9 and *Mr* 15–150 kDa [21]. The average between-gel matched percentage was 64% (61–67%) among invasive NFPA gels, and 67% (61–69%) among non-invasive NFPA gels. The positional deviation of the matched-spots was 2.05 ± 0.89 mm in the IEF direction and 1.41 ± 0.65 mm in the SDS-PAGE direction. For each sample, the average correlation coefficient (*r*) of the normalized volumes for

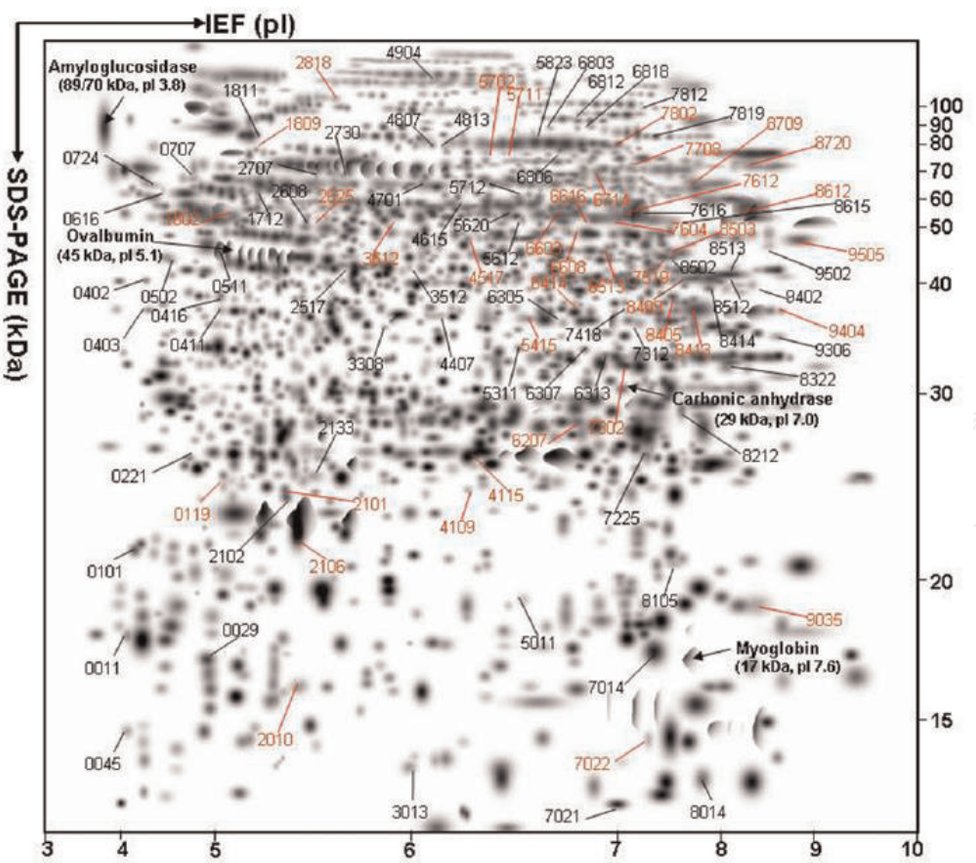

Figure 2.
2DGE map with labeled 4 standard protein markers and 103 spots containing DEPs. IEF was carried out with 18-cm IPGStrip pH 3–10 NL. SDS-PAGE was carried out with 12% polyacrylamide gel. The red means downregulated protein spot in invasive NFPAs relative to noninvasive NFPAs. The black means upregulated spot in invasive NFPAs relative to noninvasive NFPAs. Reproduced from Zhan et al. [5], with copyright permission from Wiley-VCH, copyright year 2014.

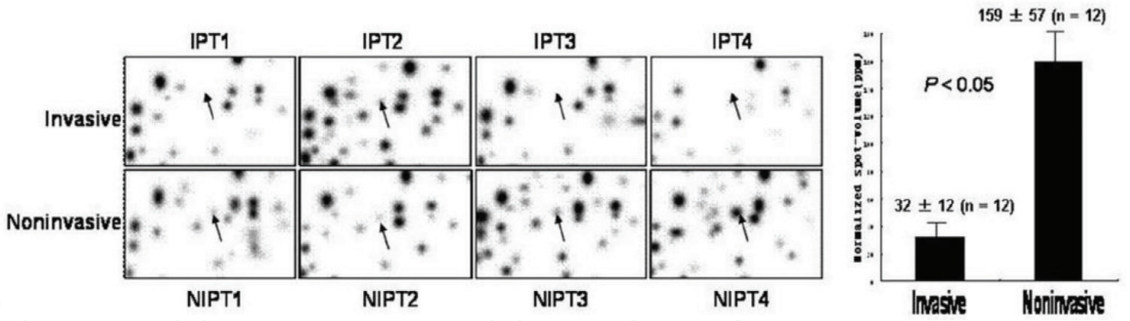

Figure 3.
A presentative differential protein spots between invasive and non-invasive NFPAs (Spot-2010). IPT: Invasive pituitary tumor. NIPT: Non-invasive pituitary tumor. Reproduced from Zhan et al. [5], with copyright permission from Wiley-VCH, copyright year 2014.

between-gel matched-spots was 0.74 (range, 0.59–0.83), with a best-fit line of: $y = 0.8685x + 0.0804$ ($r = 0.87$; $n = 811$). The normalized spot volumes between 12 invasive NFPA gels and 12 non-invasive NFPA gels were compared to determine a differential protein spot with at least 3-fold change and $p < 0.05$. For example, Spot-2010 was identified as differential protein spots downregulated in invasive NFPAs compared to non-invasive NFPAs (**Figure 3**). With the same approach, 103 differential spots were identified, including 64 upregulated and 39 downregulated protein spots in invasive NFPAs relative to non-invasive NFPAs (**Table 1** and **Figure 1**). It clearly demonstrated that the proteome was significantly different between invasive and non-invasive NFPAs.

Furthermore, each DEP in the differential spot was identified with MS [26]. For MALDI-TOF-MS PMF analysis, all interfering masses derived from contaminants including keratins, trypsin, matrix CHCA, and other unknown ones, were removed from MS spectrum of analyzed sample to obtain a corrected mass list for PMF data (**Figure 4**). Those nine masses labeled in **Figure 4B** were used with MASCOT PMF search tool to search Swiss-Prot database, and matched to the corresponding tryptic peptides from 78 kDa glucose-regulated protein (GRP78_HUMAN; P11021) (**Figure 5**), which was the DEP identified in the differential Spot-1809. With the same method, 43 DEPs was identified with PMF analysis (**Figure 1** and **Table 1**). For LC-ESI-MS/MS analysis, the tryptic peptides were separated by LC and then sequenced by MS/MS on the qTOF MS instrument, followed by MASCOT MS/MS data search in the human Swiss-Prot database. For example, six tryptic peptides from Spot-7604 were sequenced and matched to ATP synthase subunit alpha (ATPA_HUMAN; P25705) (**Figure 6**). With the same method, 11 DEPs were identified with MS/MS data (**Figure 1** and **Table 1**). A total of 57 DEPs, including 30 upregulated and 27 downregulated, were identified in invasive compared to non-invasive NFPAs (**Table 1**).

3.2 Functional characteristics of DEPs identified in invasive relative to noninvasive NFPAs

A total of 54 DEPs out of 57 DEPs were eligible for GO analysis to identify the significant BPs, CCs, and MFs, which are further grouped with hierarchical cluster into to functional clusters (**Table 2**). It clearly demonstrated those DEPs participated in multiple biological functions to associate with NFPA invasiveness, including peptidase and proteolysis, nucleotide metabolism, mitochondrial functions and oxidative stress, and protein kinase and cell signaling.

A total of 54 DEPs out of 57 DEPs were accepted for IPA pathway-network analysis to identify significant molecular networks and signaling pathways and

SSP	Swiss-Prot No.	Protein name	Mr (kDa)		pI		Fold
			Exp.	Theor.	Exp.	Theor.	
0011	Q00535	Cyclin-dependent kinase 5	17.56	33.74	4.04	7.57	13.6
0045	P04434	Ig kappa chain V-III region VH (fragment)	14.35	12.86	4.04	5.63	10.2
0029	P00742/ Q8N4Z0	Chain 1: factor X light chain/putative Ras-related protein Rab-42	16.72	54.73/ 11.59	4.90	5.68/ 5.84	3.0
0101	P23297	Protein S100-A1	21.07	10.54	4.12	4.39	18.6
0411*	P04264	Keratin, type II cytoskeletal 1	37.57	66.17	5.05	8.15	5.4
0221	Q5JXM2	Methyltransferase-like protein 24	25.65	41.87	4.71	9.41	4.6
0416	P01040	Cystatin-A	39.04	11.00	5.04	5.38	4.6
0402	Q14314	Fibroleukin	40.94	50.82	4.24	7.08	7.7
0511	P08779/ P04040	Cytokeratin 16/catalase	45.70	51.27/ 59.95	4.89	4.98/ 6.90	16.0
1712	P56817	Beta-secretase 1	61.24	56.36	5.25	5.24	8.5
2608	P78536	Disintegrin and metalloproteinase domain-containing protein 17	52.29	94.56	5.48	5.5	3.5
2133	Q9BYM8	RanBP-type and C3HC4-type zinc finger-containing protein 1	24.67	59.35	5.52	5.47	6.5
2730	Q8N3R9	MAGUK p55 subfamily member 5	68.52	77.53	5.62	5.77	3.2
2707	Q9Y3B9	RRP15-like protein	66.85	31.64	5.53	5.39	3.6
3308	P29466	Caspase-1	35.79	45.81	5.86	5.63	4.0
3013	P07108	Acyl-CoA-binding protein	13.27	10.04	5.98	6.12	3.5
3512	A2VDF0	Fucose mutarotase	42.54	16.93	5.98	5.49	14.4
4407	Q9UIY3	RWD domain-containing protein 2A	37.06	34.21	6.13	6.01	24.3
4701	Q99797	Mitochondrial intermediate peptidase	65.37	81.38	6.04	6.6	12.4
4615	Q96BJ3	Axin interactor, dorsalization- associated protein	56.24	35.17	6.25	6.13	3.4
4807	Q16891	Mitochondrial inner membrane protein	80.13	84.03	6.09	6.08	10.6
7014*	P18988	Hemoglobin beta-2 chain (PANLE)	16.98	15.93	7.33	7.25	3.4
7021*	P06576	ATP synthase subunit beta	12.29	56.56	6.98	5.26	4.2
6313	Q8NA31	Coiled-coil domain-containing protein 79	33.06	84.55	6.92	7.29	3.2
8512	Q8N823	Zinc finger protein 611	41.66	81.39	−1.00	9.16	37.4
8513	Q9Y6N3	Calcium-activated chloride channel regulator family member 3	42.45	30.29	−1.00	8.42	3.2
8212*	Q9P267/ P01834	Methyl-CpG-binding domain protein 5/ Ig kappa chain C region	28.38	159.90/ 11.61	−1.00	9.17/ 5.58	7.8
7616*	Q9P267	Methyl-CpG-binding domain protein 5	55.37	16.12	7.14	9.17	6.1
1602*	A4FU49	SH3 domain-containing protein 21	53.77	70.52	5.13	5.6	−7.4
2010	P60983	Glia maturation factor beta	15.82	16.87	5.45	5.19	−5.0
2106	P01241/ P02792	Chain 1:somatotropin/ferritin light chain	21.87	24.85/ 20.06	5.44	5.29/ 5.51	−5.9
1809	P11021	78 kDa glucose-regulated protein	78.19	72.4	5.24	5.07	−4.6
2101	P01241	Chain 1: somatotropin	23.95	24.85	5.38	5.29	−11.1

SSP	Swiss-Prot No.	Protein name	Mr (kDa)		pI		Fold
			Exp.	Theor.	Exp.	Theor.	
2625	P07332	Tyrosine-protein kinase Fes/Fps	52.98	94.12	5.54	6.27	−7.6
4517	Q8TB05	UBA-like domain-containing protein 1	47.39	19.06	6.26	6.14	−5.6
3612	Q96QD5	DEP domain-containing protein 7	50.55	58.62	5.88	7.62	−4.6
5711	P38405	Guanine nucleotide-binding protein G (olf) subunit alpha	73.36	44.79	6.49	6.23	−4.1
5415	A6NHL2	Tubulin alpha chain-like 3	36.72	50.68	6.56	5.68	−10.7
6207*	P37285	Kinesin light chain 1	27.69	63.74	6.78	5.73	−11.6
5702	P42704	Leucine-rich motif-containing protein, mitochondrial	73.4	159	6.35	5.81	−5.8
6414	Q9UL42	Paraneoplastic antigen Ma2	38.19	41.71	6.8	4.84	−10.3
6513	Q9UPQ3	Arf-GAP with GTPase, ANK repeat and PH domain-containing protein 1	44.44	95.38	6.91	8.18	−17.9
6608	Q7Z3I7/ Q9Y6G9	Zinc finger protein 572/cytoplasmic dynein 1 light intermediate china 1	48.91	63.12/ 56.54	6.75	8.32/ 6.01	−7.3
6603	Q9HD45	Transmembrane 9 superfamily member 3	53.47	68.58	6.68	6.83	−22.5
6616*	P01859	Ig gamma-2 chain C region	52.36	35.9	6.87	7.66	−33.0
7022*	P02080	Hemoglobin beta-C	14.09	15.68	7.27	11.58	−13.8
7604*	P25705	ATP synthase subunit alpha, mitochondrial	53.63	59.83	6.99	9.16	−94.3
7302*	Q96CN7	Isochorismatase domain-containing protein 1	32.25	32.5	6.99	6.96	−3.9
7519	Q99542	Chain 1: matrix metalloproteinase-19	43.84	57.36	7.45	7.22	−7.0
7802	Q96KP1	Exocyst complex component 2	80.76	105.1	6.98	6.46	−16.3
7708	Q02338	D-beta-hydroxybutyrate dehydrogenase, mitochondrial	72.25	38.53	7.11	9.11	−4.9
8503	Q9NPI8	Fanconi anemia group F protein	44.22	42.46	7.53	9.11	−8.0
8405	P17066	Heat shock 70 kDa protein 6	38.49	71.44	7.55	5.81	−25.6
8409	P25101	Endothelin-1 receptor	41.13	49.89	−1.00	8.73	−7.6

**It was identified with LC-ESI-MS/MS, and the others with MALDI-TOF-PMF.*
Fold (+) means that it is upregulated in invasive relative to noninvasive NFPAs. Fold (−) means that it is downregulated in invasive relative to noninvasive NFPAs. Exp. pI = −1.00 means that it was out of the pI range of standard markers. Reproduced from Zhan et al. [5], with copyright permission from Wiley-VCH, copyright year 2014.

Table 1.
Differentially expressed proteins between invasive and non-invasive NFPAs identified with 2DGE and mass spectrometry (fold > 3-fold or < −3-fold).

molecular networks. Three molecular networks were identified (**Figure 7**). The hub molecules among those three molecular networks included ATPase, MAPK, ERK, ERK1/2, p38, Jnk, NFkB, AKT, PKA, PKC, EGFR, K-RAS, insulin, UBC, CCND1, IFNG, NFYB, ESR1, CDK5, calmodulin, and S100A1, which are obviously associated with cancer biological systems. About 19 statistically significant canonical pathways were minded from DEPs data (**Figure 8**), including superoxide radical degradation, mitochondrial dysfunction, eNOS signaling, inhibition of matrix metalloprotease, CDK5 signaling, endoplasmic reticulum stress pathway, ketolysis, ketogenesis, TR/RXR activation, amyloid processing, endothelin-1 signaling,

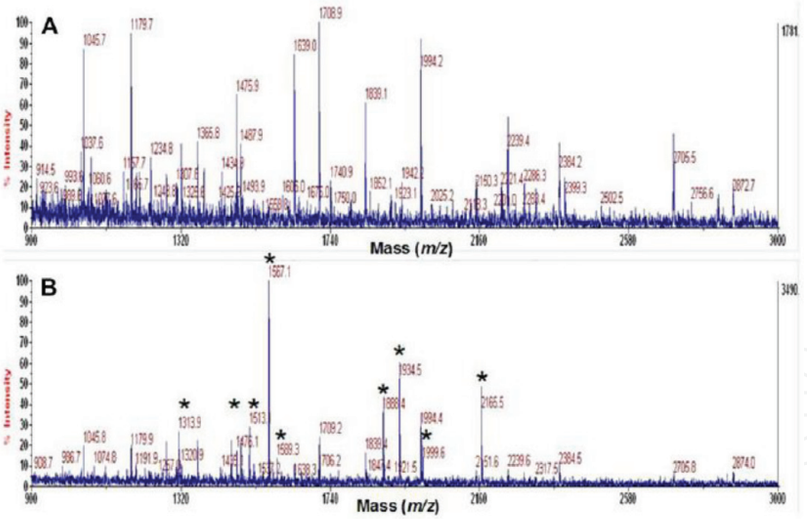

Figure 4.
*All interfering masses from contaminants derived from the margin blank gel on a silver-stained 2D gel map (A) were removed from MALDI-TOF-MS spectrum derived from the proteins in Spot-1809 (B) to obtain a corrected mass list for PMF data that were labeled as the symbol *. Reproduced from Zhan et al. [5], with copyright permission from Wiley-VCH, copyright year 2014.*

A. Summary of Mascot search result

```
User            : Xianquan Zhan
Email           : yjzhan2011@gmail.com
Search title    : Spot-1809
Database        : SwissProt 2013_08 (540732 sequences; 192091492 residues)
Taxonomy        : Homo sapiens (human) (20267 sequences)
Timestamp       : 29 Aug 2013 at 07:07:51 GMT
Top Score       : 119 for GRP78_HUMAN, 78 kDa glucose-regulated protein OS=Homo sapiens GN=HSPA5 PE=1 SV=2
```

Mascot Score Histogram

Protein score is -10*Log(P), where P is the probability that the observed match is a random event.
Protein scores greater than 56 are significant (p<0.05).

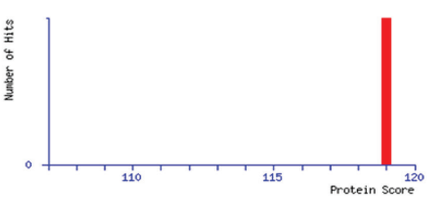

B. Peptides detected by MALDI-TOF-MS

Start-End	Peptide	Observed [M + H]$^+$	Theoretical [M + H]$^+$	Missed cleavage site	Matched
61–74	R.ITPSYVAFTPEGER.L	1567.1409	1567.1336	0	+
165–181	K.VTHAVVTVPAYFNDAQR.Q	1888.4110	1888.4037	0	+
307–324	R.IEIESFYEGEDFSETLTR.A	2165.5073	2165.5000	0	+
325–336	R.AKFEELNMDLFR.S	1513.0857	1513.0784	1	+
327–336	K.FEELNMDLFR.S	1313.9114	1313.9041	0	+
353–367	K.KSDIDEIVLVGGSTR.I	1589.2327	1589.2254	1	+
354–367	K.SDIDEIVLVGGSTR.I	1461.1272	1461.1199	0	+
475–492	K.DNHLLGTFDLTGIPPAPR.G	1934.4548	1934.4475	0	+
493–510	R.GVPQIEVTFEIDVNGILR.V	1999.5542	1999.5469	0	+

C. Matched peptides (Bold) in the amino acid sequence of 78 kDa glucose-regulated protein (GRP78_HUMAN) with a 17% coverage

```
   1 MKLSLVAAML LLLSAARAEE EDKKEDVGTV VGIDLGTTYS CVGVFKNGRV EIIANDQGNR ITPSYVAFTP EGERLIGDAA KNQLTSNPEN
  91 TVFDAKRLIG RTWNDPSVQQ DIKFLPFKVV EKKTKPYIQV DIGGGQTKTF APEEISAMVL TKMKETAEAY LGKKVTHAVV TVPAYFNDAQ
 181 RQATKDAGTI AGLNVMRIIN EPTAAAIAYG LDKREGEKNI LVFDLGGGTF DVSLLTIDNG VFEVVATNGD THLGGEDFDQ RVMEHFIKLY
 271 KKKTGKDVRK DNRAVQKLRR EVEKAKRALS SQHQARIEIE SFYEGEDFSE TLTRAKFEEL NMDLFRSTMK PVQKVLEDSD LKKSDIDEIV
 361 LVGGSTRIPK IQQLVKEFFN GKEPSRGINP DEAVAYGAAV QAGVLSGDQD TGDLVLLDVC PLTLGIETVG GVMTKLIPRN TVVPTKKSQI
 451 FSTASDNQPT VTIKVYEGER PLTKDNHLLG TFDLTGIPPA PRGVPQIEVT FEIDVNGILR VTAEDKGTGN KNKITITNDQ NRLTPEEIER
 541 MVNDAEKFAE EDKKLKERID TRNELESYAY SLKNQIGDKE KLGGKLSSED KETMEKAVEE KIEWLESHQD ADIEDFKAKK KELEEIVQPI
 631 ISKLYGSAGP PPTGEEDTAE KDEL
```

Figure 5.
Mascot search results from PMF data (Spot-1809). Modified from Zhan et al. [5], with copyright permission from Wiley-VCH, copyright year 2014.

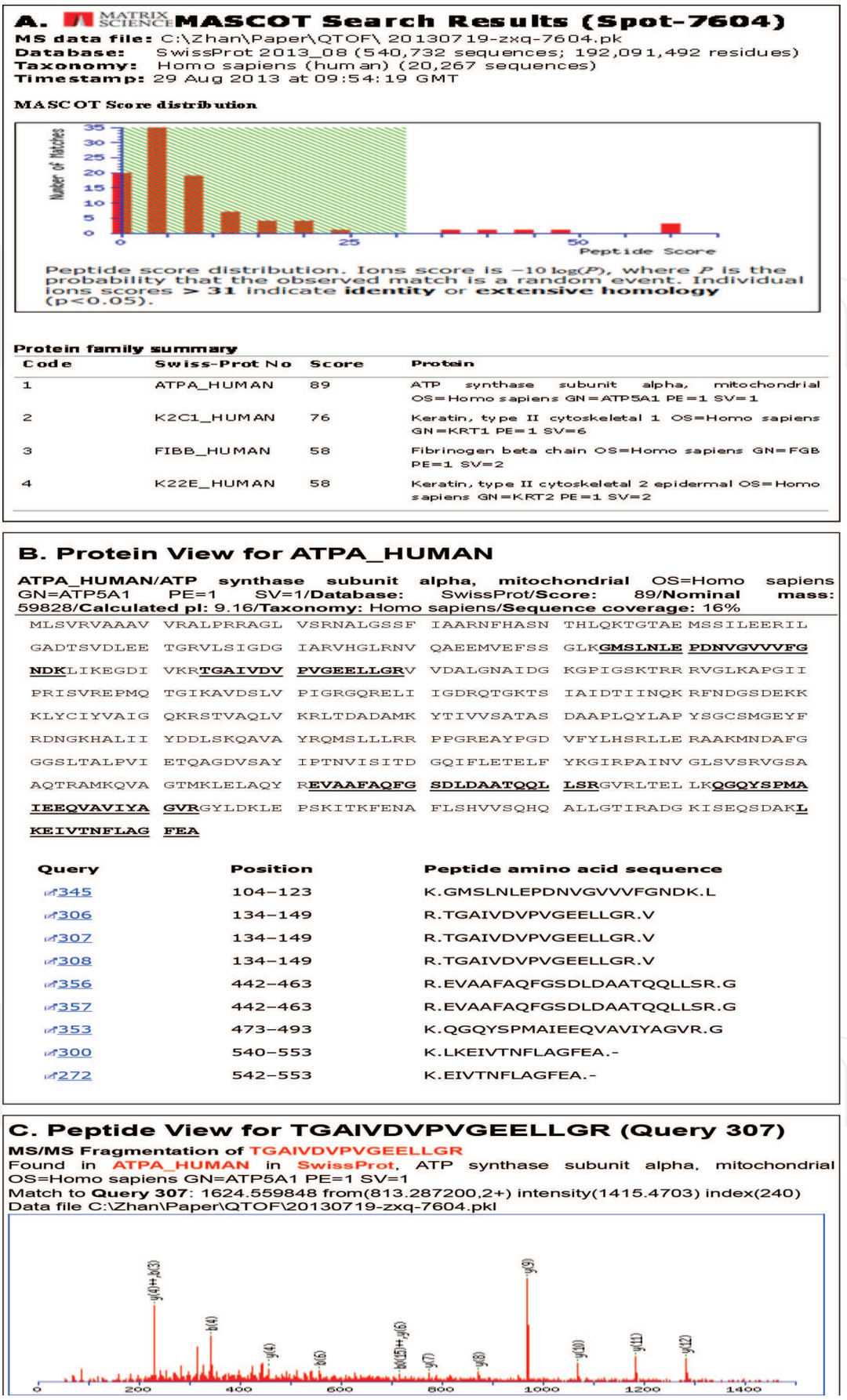

A. MASCOT Search Results (Spot-7604)

MS data file: C:\Zhan\Paper\QTOF\ 20130719-zxq-7604.pk
Database: SwissProt 2013_08 (540,732 sequences; 192,091,492 residues)
Taxonomy: Homo sapiens (human) (20,267 sequences)
Timestamp: 29 Aug 2013 at 09:54:19 GMT

MASCOT Score distribution

Peptide score distribution. Ions score is $-10\log(P)$, where P is the probability that the observed match is a random event. Individual ions scores **> 31** indicate **identity** or **extensive homology** ($p<0.05$).

Protein family summary

Code	Swiss-Prot No	Score	Protein
1	ATPA_HUMAN	89	ATP synthase subunit alpha, mitochondrial OS=Homo sapiens GN=ATP5A1 PE=1 SV=1
2	K2C1_HUMAN	76	Keratin, type II cytoskeletal 1 OS=Homo sapiens GN=KRT1 PE=1 SV=6
3	FIBB_HUMAN	58	Fibrinogen beta chain OS=Homo sapiens GN=FGB PE=1 SV=2
4	K22E_HUMAN	58	Keratin, type II cytoskeletal 2 epidermal OS=Homo sapiens GN=KRT2 PE=1 SV=2

B. Protein View for ATPA_HUMAN

ATPA_HUMAN/ATP synthase subunit alpha, mitochondrial OS=Homo sapiens GN=ATP5A1 PE=1 SV=1/**Database:** SwissProt/**Score:** 89/**Nominal mass:** 59828/**Calculated pI:** 9.16/**Taxonomy:** Homo sapiens/**Sequence coverage:** 16%

MLSVRVAAAV VRALPRRAGL VSRNALGSSF IAARNFHASN THLQKTGTAE MSSILEERIL
GADTSVDLEE TGRVLSIGDG IARVHGLRNV QAEEMVEFSS GLK**GMSLNLE** **PDNVGVVVFG**
NDKLIKEGDI VKR**TGAIVDV** **PVGEELLGR**V VDALGNAIDG KGPIGSKTRR RVGLKAPGII
PRISVREPMQ TGIKAVDSLV PIGRGQRELI IGDRQTGKTS IAIDTIINQK RFNDGSDEKK
KLYCIYVAIG QKRSTVAQLV KRLTDADAMK YTIVVSATAS DAAPLQYLAP YSGCSMGEYF
RDNGKHALII YDDLSKQAVA YRQMSLLLRR PPGREAYPGD VFYLHSRLLE RAAKMNDAFG
GGSLTALPVI ETQAGDVSAY IPTNVISITD GQIFLETELF YKGIRPAINV GLSVSRVGSA
AQTRAMKQVA GTMKLELAQY R**EVAAFAQFG** **SDLDAATQQL** **LSR**GVRLTEL LK**QGQYSPMA**
IEEQVAVIYA **GVR**GYLDKLE PSKITKFENA FLSHVVSQHQ ALLGTIRADG KISEQSDAK**L**
KEIVTNFLAG **FEA**

Query	Position	Peptide amino acid sequence
345	104–123	K.GMSLNLEPDNVGVVVFGNDK.L
306	134–149	R.TGAIVDVPVGEELLGR.V
307	134–149	R.TGAIVDVPVGEELLGR.V
308	134–149	R.TGAIVDVPVGEELLGR.V
356	442–463	R.EVAAFAQFGSDLDAATQQLLSR.G
357	442–463	R.EVAAFAQFGSDLDAATQQLLSR.G
353	473–493	K.QGQYSPMAIEEQVAVIYAGVR.G
300	540–553	K.LKEIVTNFLAGFEA.-
272	542–553	K.EIVTNFLAGFEA.-

C. Peptide View for TGAIVDVPVGEELLGR (Query 307)

MS/MS Fragmentation of TGAIVDVPVGEELLGR
Found in **ATPA_HUMAN** in **SwissProt**, ATP synthase subunit alpha, mitochondrial OS=Homo sapiens GN=ATP5A1 PE=1 SV=1
Match to **Query 307**: 1624.559848 from(813.287200,2+) intensity(1415.4703) index(240)
Data file C:\Zhan\Paper\QTOF\20130719-zxq-7604.pkl

Figure 6.
Mascot search results from a representative LC-ESI-MS/MS data from proteins in Spot-7604. Modified from Zhan et al. [5], with copyright permission from Wiley-VCH, copyright year 2014.

Category	Term	Count	P-value	Proteins (DEPs)
Annotation Cluster 1				
GOTERM_BP_FAT	Regulation of protein kinase cascade	5	5.56E − 03	P29466, Q96BJ3, P00742, P01241, P04040
GOTERM_BP_FAT	Positive regulation of signal transduction	5	1.00E − 02	P29466, P00742, P01241, P04040, P78536
GOTERM_BP_FAT	Positive regulation of protein kinase cascade	4	1.22E − 02	P29466, P00742, P01241, P04040
GOTERM_BP_FAT	Positive regulation of cell communication	5	1.45E-02	P29466, P00742, P01241, P04040, P78536
Annotation Cluster 2				
GOTERM_MF_FAT	Endopeptidase activity	6	3.99E − 03	P29466, P00742, Q99542, Q99797, P56817, P78536
GOTERM_MF_FAT	Peptidase activity, acting on L-amino acid peptides	6	1.89E − 02	P29466, P00742, Q99542, Q99797, P56817, P78536
GOTERM_MF_FAT	Peptidase activity	6	2.25E − 02	P29466, P00742, Q99542, Q99797, P56817, P78536
GOTERM_BP_FAT	Proteolysis	8	2.92E − 02	P29466, P00742, Q99542, Q9BYM8, Q99797, P04264, P56817, P78536
GOTERM_MF_FAT	Metalloendopeptidase activity	3	3.53E − 02	Q99542, Q99797, P78536
Annotation Cluster 3				
GOTERM_CC_FAT	Mitochondrial lumen	5	3.29E − 03	Q02338, P06576, P42704, P25705, Q99797
GOTERM_CC_FAT	Mitochondrial matrix	5	3.29E − 03	Q02338, P06576, P42704, P25705, Q99797
GOTERM_CC_FAT	Mitochondrial part	7	5.08E − 03	Q02338, P06576, P42704, P25705, Q99797, P04040, Q16891
GOTERM_CC_FAT	Organelle envelope	7	6.20E − 03	Q02338, P06576, P42704, P25705, P04040, P25101, Q16891
GOTERM_CC_FAT	Envelope	7	6.29E − 03	Q02338, P06576, P42704, P25705, P04040, P25101, Q16891
GOTERM_CC_FAT	Organelle inner membrane	5	1.20E − 02	Q02338, P06576, P42704, P25705, Q16891
GOTERM_CC_FAT	Mitochondrial envelope	5	2.67E − 02	Q02338, P06576, P25705, P04040, Q16891
GOTERM_CC_FAT	Organelle membrane	8	2.68E − 02	Q02338, P06576, P42704, P25705, P11021, P04040, P25101, Q16891
GOTERM_CC_FAT	Mitochondrial membrane part	3	4.58E − 02	P06576, P25705, Q16891
GOTERM_CC_FAT	Mitochondrial inner membrane	4	5.06E − 02	Q02338, P06576, P25705, Q16891
Annotation Cluster 4				
GOTERM_BP_FAT	Response to organic substance	7	1.63E − 02	P29466, Q00535, P01241, P38405, P25101, P17066, P78536
Annotation Cluster 5				

Category	Term	Count	P-value	Proteins (DEPs)
GOTERM_BP_FAT	Proteolysis	8	2.92E − 02	P29466, P00742, Q99542, Q9BYM8, Q99797, P04264, P56817, P78536
GOTERM_BP_FAT	Protein processing	3	4.13E − 02	P29466, Q99797, P04264
GOTERM_BP_FAT	Protein maturation	3	4.81E − 02	P29466, Q99797, P04264
Annotation Cluster 6				
GOTERM_BP_FAT	Response to alkaloid	3	1.05E − 02	Q00535, P38405, P25101
GOTERM_BP_FAT	Response to organic substance	7	1.63E − 02	P29466, Q00535, P01241, P38405, P25101, P17066, P78536
GOTERM_BP_FAT	Positive regulation of molecular function	6	2.56E − 02	Q00535, P01241, P38405, P04040, P25101, P78536
GOTERM_BP_FAT	Positive regulation of protein kinase activity	4	2.61E − 02	Q00535, P01241, P25101, P78536
GOTERM_BP_FAT	Positive regulation of protein amino acid phosphorylation	3	2.71E − 02	P01241, P25101, P78536
GOTERM_BP_FAT	Positive regulation of kinase activity	4	2.86E − 02	Q00535, P01241, P25101, P78536
GOTERM_BP_FAT	Positive regulation of transferase activity	4	3.15E − 02	Q00535, P01241, P25101, P78536
GOTERM_BP_FAT	Positive regulation of phosphorylation	3	3.18E − 02	P01241, P25101, P78536
GOTERM_BP_FAT	Positive regulation of phosphate metabolic process	3	3.36E − 02	P01241, P25101, P78536
GOTERM_BP_FAT	Positive regulation of phosphorus metabolic process	3	3.36E − 02	P01241, P25101, P78536
GOTERM_BP_FAT	Response to organic cyclic substance	3	4.74E − 02	Q00535, P38405, P25101
Annotation Cluster 7				
GOTERM_MF_FAT	Purine ribonucleotide binding	11	2.91E − 02	Q9Y6G9, P06576, P07332, Q8N4Z0, Q00535, P25705, Q9UPQ3, P11021, P38405, P17066, A6NHL2
GOTERM_MF_FAT	Ribonucleotide binding	11	2.91E − 02	Q9Y6G9, P06576, P07332, Q8N4Z0, Q00535, P25705, Q9UPQ3, P11021, P38405, P17066, A6NHL2
GOTERM_MF_FAT	Purine nucleotide binding	11	3.80E − 02	Q9Y6G9, P06576, P07332, Q8N4Z0, Q00535, P25705, Q9UPQ3, P11021, P38405, P17066, A6NHL2
GOTERM_MF_FAT	Nucleotide binding	12	4.37E − 02	Q9Y6G9, P06576, P07332, Q8N4Z0, Q00535, P25705, Q9UPQ3, P11021, P38405, P04040, P17066, A6NHL2
Annotation Cluster 8				

Category	Term	Count	P-value	Proteins (DEPs)
GOTERM_BP_FAT	Proteolysis	8	2.92E − 02	P29466, P00742, Q99542, Q9BYM8, Q99797, P04264, P56817, P78536
Annotation Cluster 9				
GOTERM_MF_FAT	Calcium ion binding	7	4.37E − 02	P06576, P00742, Q9Y6N3, Q99542, P23297, P11021, Q99797
Annotation Cluster 10				
GOTERM_CC_FAT	Cell surface	5	1.45E − 02	P06576, P00742, P11021, P56817, P78536

Modified from Zhan et al. [5], with copyright permission from Wiley-VCH, copyright year 2014.

Table 2.
The functional categories of 54 DEPs identified by GO analysis.

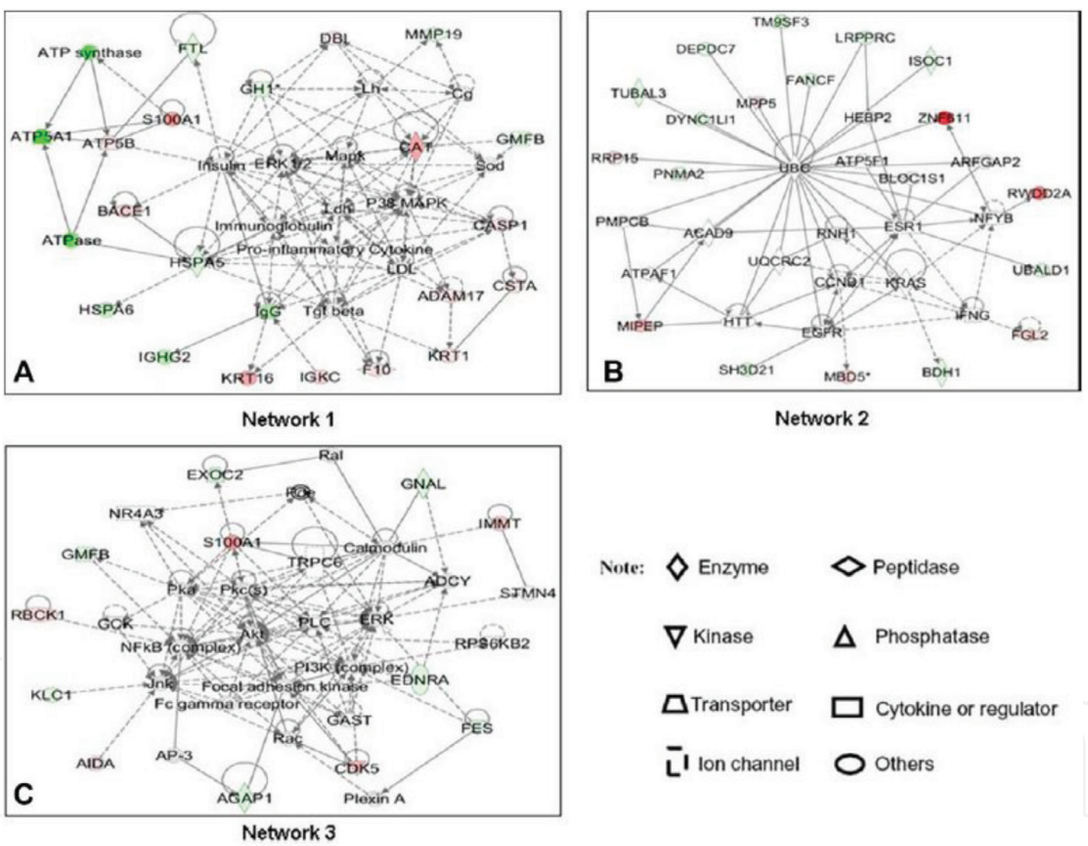

Figure 7.
Significant molecular networks changed in invasive NFPAs. (A) Network 1 functioned in inflammatory disease and inflammatory response. (B) Network 2 functioned in tumor morphology, cancer, cell-to-cell signaling, and interaction. (C) Network 3 functioned in tissue morphology, nervous system development and function, and organismal development. A black solid edge means a direct relationship. A black unsolid edge means an indirect relationship. A red node means upregulated proteins. A green node means downregulated proteins. Reproduced from Zhan et al. [5], with copyright permission from Wiley-VCH, copyright year 2014.

semaphoring signaling in neurons, axonal guidance signaling, neuregulin signaling, and primary immunodeficiency signaling [5]. Also, 10 significant toxicological events were identified with those DEP data, including mitochondrial dysfunction, decreased permeability transition/transmembrane potential/depolarization of mitochondria and mitochondrial membrane, anti-oxidative response panel, and TR/RXR activation. Our previous studies also revealed that MAPK-signaling

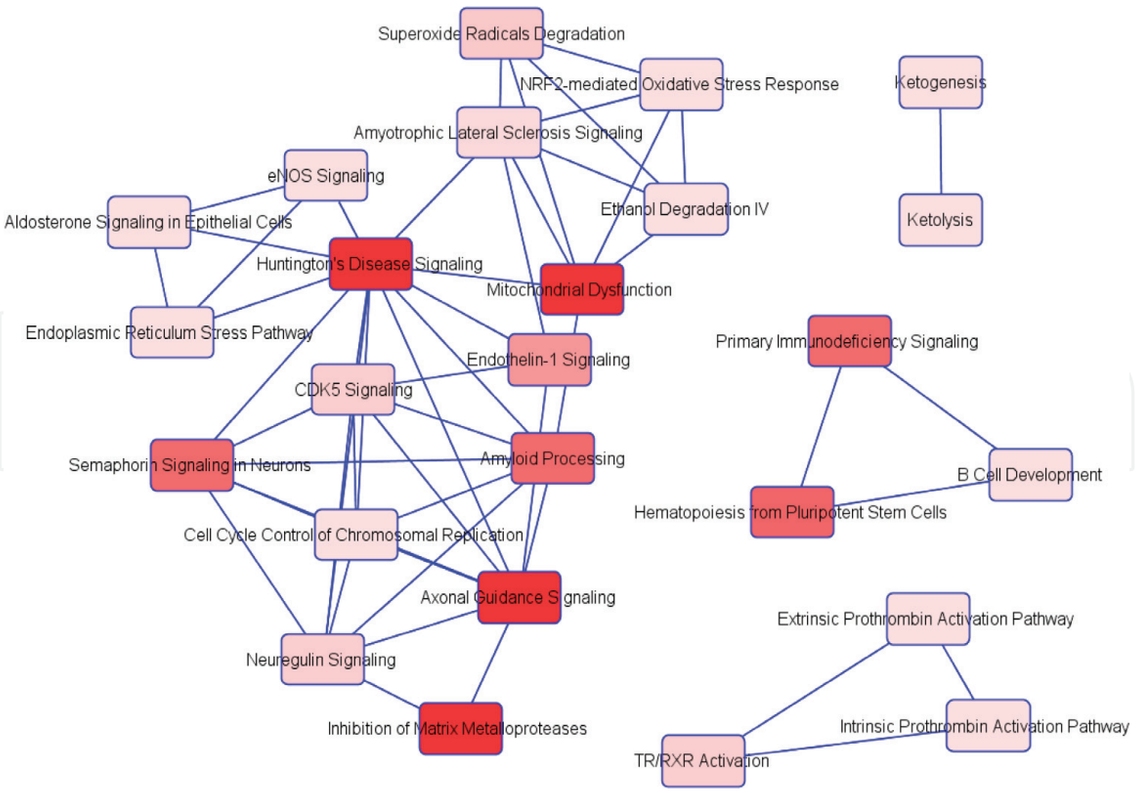

Figure 8.
Statistically significant canonical pathways to involve DEPs in invasive NFPAs. Modified from Zhan et al. [5], with copyright permission from Wiley-VCH, copyright year 2014.

abnormality, oxidative stress, mitochondrial dysfunction, and TR/RXR activation are significantly associated with NFPAs and invasive NFPAs [27], and the changed molecule-pattern in each pathway-system was different between NFPA and invasive NFPA, which might contribute to the pathological processes of invasive NFPAs. Furthermore, ketogenesis and ketolysis, proteolysis abnormality, amyloid processing, and CDK5 signaling abnormality were also obviously related to invasive NAPFs. Therefore MAPK-signaling abnormality, mitochondrial dysfunction, TR/RXR activation, oxidative stress, proteolysis abnormality, CDK5 signaling abnormality, ketogenesis and ketolysis, and amyloid processing were significantly associated with invasive characteristics of invasive NFPAs, and pathway-network-based molecule patterns benefit to identify reliable biomarkers for invasive NFPAs.

4. Conclusions

Invasiveness is serious clinical problem in human pituitary adenomas. It is necessary to clarify its molecular mechanisms and discover effective biomarkers to guide management of invasive NFPAs. This 2DGE-based comparative proteomics and bioinformatics successfully identified proteomic variation profiling and pathway-network changes in human invasive NFPAs compared to noninvasive NFPAs, found 103 differential protein spots (64 upregulated and 39 downregulated) in invasive versus noninvasive NFPA 2DE maps, and identified 57 DEPs (30 upregulated and 27 downregulated), which are significantly involved in pathogenetic process of invasive NFPAs, with altered pathway networks including MAPK-signaling abnormality, oxidative stress, mitochondrial dysfunction, ketogenesis and ketolysis, CDK5 signaling abnormality, TR/RXR activation, proteolysis abnormality, and amyloid processing. Moreover, some important hub-molecules were identified to associate with cancer biological processes, including ATPase,

MAPK, ERK, ERK1/2, p38, Jnk, NFkB, AKT, PKA, PKC, EGFR, K-RAS, insulin, UBC, CCND1, IFNG, NFYB, ESR1, CDK5, calmodulin, and S100A1. Those DEPs, changed pathway networks, and hub-molecules provided new insights into molecular mechanisms of NFPA invasiveness, and important resource for discovery of effective biomarkers to guide the management of invasive NFPAs.

Acknowledgements

The authors acknowledge the financial supports from the Hunan Provincial "Hundred Talent Plan" program (to X.Z.), the Xiangya Hospital Funds for Talent Introduction (to X.Z.), the Hunan Provincial Natural Science Foundation of China (Grant No. 14JJ7008 to X.Z.), China "863" Plan Project (Grant No. 2014AA020610-1 to X.Z.), and the National Natural Science Foundation of China (Grant No. 81572278 and 81272798 to X.Z.). The scientific contributions of Dr. Dominic M. Desiderio from University of Tennessee Health Science Center were also acknowledged.

Conflict of interest

We declare that we have no financial and personal relationships with other people or organizations.

Author's contributions

X.Z. conceived the concept, designed the book chapter, and wrote and critically revised the book chapter, coordinated and was responsible for the correspondence work and financial support. X.H.Z and X.W participated in experiments. X.H.Z edited the English language. All authors approved the final manuscript.

Acronyms and abbreviations

BP	biological processes
CC	cellular components
DEP	differentially expressed protein
ESI	electrospray ionization
FPA	functional pituitary adenomas
IEF	isoelectric focusing
IPA	ingenuity pathway analysis
IPG	immobilized pH gradient
LC	liquid chromatography
MALDI	matrix-assisted laser desorption/ionization
MF	molecular functions
Mr	relative mass
MRI	magnetic resonance imaging
MS	mass spectrometry
MS/MS	tandem mass spectrometry
NFPA	nonfunctional pituitary adenoma
pI	isoelectric point
PMF	peptide mass fingerprint
SDS-PAGE	sodium dodecyl sulfate-polyacrylamide gel electrophoresis
TOF	time-of-flight
2DGE	two-dimensional gel electrophoresis

Author details

Xianquan Zhan[1,2*], Xiaohan Zhan[1,2] and Xiaowei Wang[1,2]

1 Key Laboratory of Cancer Proteomics of Chinese Ministry of Health, Xiangya Hospital, Central South University, Changsha, P.R. China

2 State Local Joint Engineering Laboratory for Anticancer Drugs, Xiangya Hospital, Central South University, Changsha, P.R. China

*Address all correspondence to: yjzhan2011@gmail.com

References

[1] Hussaini IM, Trotter C, Zhao Y, Abdel-Fattah R, Amos S, Xiao A, et al. Matrix metalloproteinase-9 is differentially expressed in nonfunctioning invasive and noninvasive pituitary adenomas and increases invasion in human pituitary adenoma cell line. The American Journal of Pathology. 2007;**170**:356-365. DOI: 10.2353/ajpath.2007.060736

[2] Martins AN, Hayes GJ, Kempe LG. Invasive pituitary adenomas. Journal of Neurosurgery. 1965;**22**:268-276. DOI: 10.3171/jns.1965.22.3.0268

[3] Zhang X, Fei Z, Zhang W, Zhang JN, Liu WP, Fu LA, et al. Endoscopic endonasal transsphenoidal surgery for invasive pituitary adenoma. Journal of Clinical Neuroscience. 2008;**15**:241-245. DOI: 10.1016/j.jocn.2007.03.008

[4] Hashimoto N, Handa H, Yamashita J, Yamagami T. Long-term follow-up of large or invasive pituitary adenomas. Surgical Neurology. 1986;**25**:49-54. DOI: 10.1016/0090-3019(86)90114-X

[5] Zhan X, Desiderio DM, Wang X, Zhan X, Guo T, Li M, et al. Identification of the proteomic variations of invasive relative to non-invasive non-functional pituitary adenomas. Electrophoresis. 2014;**35**:2184-2194. DOI: 10.1002/elps.201300590

[6] Zhan X, Wang X, Cheng T. Human pituitary adenoma proteomics: New progresses and perspectives. Frontiers in Endocrinology. 2016;**7**:54. DOI: 10.3389/fendo.2016.00054

[7] Meij BP, Lopes MB, Ellegala DB, Alden TD, Laws ER Jr. The long-term significance of microscopic dural invasion in 354 patients with pituitary adenomas treated with transsphenoidal surgery. Journal of Neurosurgery. 2002; **96**:195-208. DOI: 10.3171/jns.2002.96.2.0195

[8] Selman WR, Laws ER Jr, Scheithauer BW, Carpenter SM. The occurrence of dural invasion in pituitary adenomas. Journal of Neurosurgery. 1986;**64**:402-407. DOI: 10.3171/jns.1986.64.3.0402

[9] Galland F, Lacroix L, Saulnier P, Dessen P, Meduri G, Bernier M, et al. Differential gene expression profiles of invasive and non-invasive non-functioning pituitary adenomas based on microarray analysis. Endocrine-Related Cancer. 2010;**17**:361-371. DOI: 10.1677/ERC-10-0018

[10] Turner HE, Nagy Z, Gatter KC, Esiri MM, Harris AL, Wass JA. Angiogenesis in pituitary adenomas—Relationship to endocrine function, treatment and outcome. Journal of Endocrinology. 2000;**165**:475-481

[11] Qian ZR, Sano T, Yoshimoto K, Asa SL, Yamada S, Mizusawa N, et al. Tumor-specific downregulation and methylation of the CDH13 (H-cadherin) and CDH1 (E-cadherin) genes correlate with aggressiveness of human pituitary adenomas. Modern Pathology. 2007;**20**: 1269-1277. DOI: 10.1038/modpathol.3800965

[12] Simpson DJ, Clayton RN, Farrell WE. Preferential loss of death associated protein kinase expression in invasive pituitary tumours is associated with either CpG island methylation or homozygous deletion. Oncogene. 2002;**21**:1217-1224. DOI: 10.1038/sj.onc.1205195

[13] Nam DH, Song SY, Park K, Kim MH, Suh YL, Lee JI, et al. Clinical significance of molecular genetic changes in sporadic invasive pituitary adenomas. Experimental & Molecular Medicine. 2001;**33**:111-116. DOI: 10.1038/emm.2001.20

[14] Farrell WE. Pituitary tumours: Findings from whole genome analyses.

Endocrine-Related Cancer. 2006;**13**: 707-716. DOI: 10.1677/erc.1.01131

[15] Zhan X, Desiderio DM. Editorial: Systems biological aspects of pituitary Tumors. Frontiers in Endocrinology. 2016;**7**:86. DOI: 10.3389/fendo.2016.00086

[16] Zhan X, Long Y. Exploration of molecular network variations in different subtypes of human non-functional pituitary adenomas. Frontiers in Endocrinology. 2016;**7**:13. DOI: 10.3389/fendo.2016.00013

[17] Hu R, Wang X, Zhan X. Multi-parameter systematic strategies for predictive, preventive and personalised medicine in cancer. The EPMA Journal. 2013;**4**:2. DOI: 10.1186/1878-5085-4-2

[18] Cheng T, Zhan X. Pattern recognition for predictive, preventive, and personalized medicine in cancer. The EPMA Journal. 2017;**8**:51-60. DOI: 10.1007/s13167-017-0083-9

[19] Lu M, Zhan X. The crucial role of multiomic approach in cancer research and clinically relevant outcomes. The EPMA Journal. 2018;**9**:77-102. DOI: 10.1007/s13167-018-0128-8

[20] Wierinckx A, Auger C, Devauchelle P, Reynaud A, Chevallier P, Jan M, et al. A diagnostic marker set for invasion, proliferation, and aggressiveness of prolactin pituitary tumors. Endocrine-Related Cancer. 2007;**14**:887-900. DOI: 10.1677/ERC-07-0062

[21] Zhan X, Desiderio DM. Comparative proteomics analysis of human pituitary adenomas: Current status and future perspectives. Mass Spectrometry Reviews. 2005;**24**: 783-813. DOI: 10.1002/mas.20039

[22] Moreno CS, Evans CO, Zhan X, Okor M, Desiderio DM, Oyesiku NM. Novel molecular signaling and classification of human clinically nonfunctional pituitary adenomas identified by gene expression profiling and proteomic analyses. Cancer Research. 2005;**65**:10214-10222. DOI: 10.1158/0008-5472.CAN-05-0884

[23] Zhan X, Huang Y, Long Y. Two-dimensional gel electrophoresis coupled with mass spectrometry methods for an analysis of human pituitary adenoma tissue proteome. Journal of Visualized Experiments. 2018;**134**:1. DOI: 10.3791/56739

[24] Zhan X, Desiderio DM. The use of variations in proteomes to predict, prevent, and personalize treatment for clinically nonfunctional pituitary adenomas. The EPMA Journal. 2010;**1**: 439-459. DOI: 10.1007/s13167-010-0028-z

[25] Liu Z, Liu Y, Fang W, Chen W, Li C, Xiao Z. Establishment of differential expression profiles from invasive and non-invasive pituitary adenomas. Journal of central south university (medical sciences). 2009;**34**:569-575. DOI: 1672-7347(2009)07-0569-07

[26] Zhan X, Desiderio DM. A reference map of a human pituitary adenoma proteome. Proteomics. 2003;**3**:699-713. DOI: 10.1002/pmic.200300408

[27] Zhan X, Desiderio DM. Signaling pathway networks mined from human pituitary adenoma proteomics data. BMC Medical Genomics. 2010;**3**:13. DOI: 10.1186/1755-8794-3-13